

Domain-wall fermions with $U(1)$ dynamical gauge fields

S. Aoki and K. Nagai

Institute of Physics, University of Tsukuba, Tsukuba, Ibaraki 305, Japan

(October 16, 2018)

Abstract

We have carried out a numerical simulation of a domain-wall model in $(2+1)$ -dimensions, in the presence of a dynamical gauge field only in an extra dimension, corresponding to the weak coupling limit of a (2-dimensional) physical gauge coupling. Using a quenched approximation we have investigated this model at $\beta_s(= 1/g_s^2) = 0.5$ (“symmetric” phase), 1.0, and 5.0 (“broken” phase), where g_s is the gauge coupling constant of the extra dimension. We have found that there exists a critical value of a domain-wall mass m_0^c which separates a region with a fermionic zero mode on the domain-wall from the one without it, in both symmetric and broken phases. This result suggests that the domain-wall method may work for the construction of lattice chiral gauge theories.

11.15Ha, 11.30Rd, 11.90.+t

I. INTRODUCTION

Construction of chiral gauge theories is one of the long-standing problems of lattice field theories. Due to the fermion doubling problems, a naively discretized lattice fermion field yields 2^d fermion particles, half of one chirality and half of the other, so that the theory becomes non-chiral [1]. Several lattice approaches have been proposed, but so far none of them have been proven to work successfully.

Kaplan has proposed a new construction of lattice chiral gauge theories via domain-wall models [2]. Starting from a vector-like gauge theory in $2k + 1$ -dimensions with a fermion mass term being a shape of a domain-wall in the (extra) $2k + 1$ -th dimension, he showed in the weak gauge coupling limit that a massless chiral state arises as a zero mode bound to the $2k$ -dimensional domain-wall while all the doublers have large masses of the lattice cut-off scale. It has been also shown that the model works well for smooth back-ground gauge fields [3,4].

Two simplified variants of the original Kaplan's domain-wall model have been proposed: an "overlap formula" [6] and a "waveguide model" [7]. Gauge fields appeared in these variants are $2k$ -dimensional and are independent of the extra $2k + 1$ -th coordinate, while those in the original model are $2k + 1$ -dimensional and depend on the extra $2k + 1$ -th coordinate. These variants work successfully for smooth back-ground gauge fields [8,9], as the original one does. Non-perturbative investigations for these variants seems easier than for the original model due to the simpler structure of gauge fields.

However it has been reported [7] that the waveguide model in the weak gauge coupling limit can not produce chiral zero modes needed to construct chiral gauge theories. In this limit, if gauge invariance were maintained, pure gauge field configurations equivalent to the unity by gauge transformation would dominate and gauge fields would become smooth. In the set-up of the waveguide model, however, $2k$ -dimensional gauge fields are non-zero only in the layers near domain-wall(waveguide), so that the gauge invariance is broken in the edge of the waveguide. Therefore, even in the weak gauge coupling limit, gauge fields are

no more smooth and becomes very “rough”, due to the gauge degrees of freedom appeared to be dynamical in this edge. As a result of the rough gauge dynamics, a new chiral zero mode with the opposite chirality to the original zero mode on the domain-wall appears in the edge, so that the fermionic spectrum inside the waveguide becomes vector-like. It has been claimed [7] that this ”rough gauge” problem also exists in the overlap formula since the gauge invariance is broken by the boundary condition at the infinity of the extra dimension [9,10]. Furthermore an equivalence between the wave-guide model and the overlap formula has been pointed out for the special case [11]. Although the claimed equivalence has been challenged in ref. [12], it is still crucial for the success of the overlap formula to solve the ”rough gauge” problem and to show the existence of a chiral zero mode in the weak gauge coupling limit.

How about original Kaplan’s model ? In this model there are two inverse gauge coupling $\beta = 1/g^2$ and $\beta_s = 1/g_s^2$, where g is the coupling constant in (physical) $2k$ -dimensions and g_s is the one in the (extra) $2k + 1$ -th dimension. Very little are known about this model except $\beta_s = 0$ case [13,14] where the spectrum seems vector-like. In the weak coupling limit, corresponding to the $g \rightarrow 0$ limit in this model, all gauge fields in the physical dimensions can be gauged away, while the gauge field in the extra dimension is still dynamical and its dynamics is controlled by β_s . Instead of the gauge degrees of freedom in the edge of the wave-guide, $2k + 1$ -th component of gauge fields represent roughness of $2k$ dimensional gauge fields. An important question is whether the chiral zero mode on the domain-wall survives in the presence of this rough dynamics. The dynamics of the gauge field in this limit is equivalent to $2k$ dimensional scalar model with L_s independent copies where L_s is the number of sites in the extra dimension. In general at large β_s such a system is in a “broken phase” where some global symmetry is spontaneously broken, while at small β_s the system is in a “symmetric” phase. Therefore there exists a critical point β_s^c , and it is likely that the phase transition at $\beta_s = \beta_s^c$ is continuous(second or higher order). The ”gauge field” becomes rougher and rougher at smaller β_s . Indeed we know that the zero modes disappears at $\beta_s = 0$ [13], while the zero mode exists at $\beta_s = \infty$ (free case). So far we

do not know the fate of the chiral zero mode in the intermediate range of the coupling β_s . There are the following 3 possibilities: (a) The chiral zero mode always exists except $\beta_s = 0$. In this case we may likely construct a lattice chiral gauge theory in both broken ($\beta_s > \beta_s^c$) and symmetric ($\beta_s < \beta_s^c$), and the continuum limits may be taken at $\beta_s = \beta_s^c$. This is the beset case for the domain-wall model. (b) The chiral zero mode exists only in the broken phase ($\beta_s > \beta_s^c$). In this case we may construct a lattice chiral gauge theory only in the broken phase via the domain-wall method. This is unsatisfactory, since the chiral gauge theory in the symmetric phase, which is an important theoretical basis for various models, can not be described via the domain-wall method. (c) No chiral zero mode survives except $\beta_s = \infty$. The original Kaplan's model can not describe lattice chiral gauge theories at all.

It is very important to determine which possibility is indeed realized in the domain-wall model. Therefore, in this paper, in order to know the fate of the chiral zero mode, we have carried out a numerical simulation of a domain-wall model in $(2 + 1)$ -dimension with a quenched $U(1)$ gauge field in the $\beta = \infty$ limit. Strictly speaking, there is no order parameter in a 2 dimensional $U(1)$ model (XY model). On a large but finite lattice, however, a behavior of the 2 dimensional model is similar to the one of a 4 dimensional scalar model. Thus, we hopefully think that useful informations about the fate of the zero mode can be obtained from such a toy model in $(2+1)$ -dimensions. In Sec.2, we have defined our domain-wall model with dynamical gauge fields. We have calculated a fermion propagator by using a kind of mean-field approximation, to show that there is a critical value of the domain-wall mass parameter above which the zero mode exist. The value of the critical mass may depend on β_s , which controls the dynamics of the gauge field. In Sec.3, we have calculated the fermion spectrum numerically using quenched approximation at $\beta_s = 0.5, 1.0, 5.0$ and at various values of domain-wall masses. We have found that at any value of three β_s there always exists the range of domain-wall mass parameter in which the chiral zero mode survives on the domain-wall. Our conclusion and some discussions are given in Sec. 4.

II. DOMAIN-WALL MODEL

A. Definition of the model

We consider a vector gauge theory in $d = (2k + 1)$ -dimension with a domain-wall mass term, which has a shape of a step function in the coordinate of an extra dimension. This domain-wall model is originally proposed by Kaplan [2], and a fermionic part of the action is reformulated by Narayanan-Neuberger [5], in terms of a $2k$ -dimensional theory. The model is defined by the action

$$S = S_G + S_F, \quad (1)$$

where S_G is the action of a dynamical gauge field, S_F is the fermionic action. S_G is given by

$$S_G = \beta \sum_{n, \mu > \nu} \sum_s \text{ReTr} [U_{\mu\nu}(n, s)] + \beta_s \sum_{n, \mu} \sum_s \text{ReTr} [U_{\mu d}(n, s)], \quad (2)$$

where μ, ν run from 1 to $2k$, n is a $2k$ -dimensional lattice point, and s is a coordinate of an extra dimension. $U_{\mu\nu}(n, s)$ is a $2k$ -dimensional plaquette and $U_{\mu d}(n, s)$ is a plaquette containing two link variables in the extra direction. β is the inverse gauge coupling for the plaquette $U_{\mu\nu}$ and β_s is the one for the plaquette $U_{\mu d}$. In general, $\beta \neq \beta_s$. The fermion action S_F on the Euclidean lattice, in terms of the $2k$ -dimensional notation, is given by

$$S_F = \frac{1}{2} \sum_{n, \mu} \sum_s \bar{\psi}_s(n) \gamma_\mu \left[U_{s, \mu}(n) \psi_s(n + \mu) - U_{s, \mu}^\dagger(n - \mu) \psi_s(n - \mu) \right] + \sum_n \sum_{s, t} \bar{\psi}_s(n) \left[M_0 P_R + M_0^\dagger P_L \right] \psi_t(n) + \frac{1}{2} \sum_{n, \mu} \sum_s \bar{\psi}_s(n) \left[U_{s, \mu}(n) \psi_s(n + \mu) + U_{s, \mu}^\dagger(n - \mu) \psi_s(n - \mu) - 2\psi_s(n) \right] \quad (3)$$

where s, t are an extra coordinates, $P_{R/L} = \frac{1}{2}(1 \pm \gamma_{2k+1})$,

$$(M_0)_{s, t} = U_{s, d}(n) \delta_{s+1, t} - a(s) \delta_{s, t} \quad (4)$$

$$(M_0^\dagger)_{s, t} = U_{s-1, d}^\dagger(n) \delta_{s-1, t} - a(s) \delta_{s, t}. \quad (5)$$

Here $U_{s,\mu}(n), U_{s,d}(n)$ ($d = 2k + 1$) are link variables connecting a site (n, s) to $(n + \mu, s)$ or $(n, s + 1)$, respectively, Because of a periodic boundary condition in the extra dimension , s, t run from $-L_s$ to $L_s - 1$, and $a(s)$ is given by

$$\begin{aligned}
 a(s) &= 1 - m_0 \operatorname{sign} \left[\left(s + \frac{1}{2} \right) \operatorname{sign} \left(L_s - s - \frac{1}{2} \right) \right] \\
 &= \begin{cases} 1 - m_0 & \left(-\frac{1}{2} < s < L_s - \frac{1}{2} \right) \\ 1 + m_0 & \left(-L_s - \frac{1}{2} < s < -\frac{1}{2} \right), \end{cases} \tag{6}
 \end{aligned}$$

where m_0 is the height of the domain-wall mass. It is easy to check that the above fermionic action is identical to the one in $(2k + 1)$ -dimensions, proposed by Kaplan [2,5].

In weak coupling limit of both β and β_s , this model becomes free theory and can be easily analyzed. In free theory at $0 < m_0 < 1$, it has been shown that a desired chiral zero mode appears on a domain-wall($s = 0$ plane) without unwanted doublers. Due to the periodic boundary condition in the extra dimension, however , a zero mode of the opposite chirality to the one on the domain-wall appears on the anti-domain-wall , $s = L_s - 1$. Overlap between two zero modes decreases exponentially at large L_s . A free fermion propagator is easily calculated and an effective action of a $(2 + 1)$ -dimensional model including the gauge anomaly and the Chern-Simons term can be obtained for smooth background gauge fields [3].

Domain-wall models, however, have not been investigated yet *non-perturbatively*. Main question is whether the chiral zero mode survives in the presence of rough gauge fields mentioned in the introduction. To answer this question we will analyze the fate of the chiral zero mode in the weak coupling limit for β . In this limit, the gauge field action S_G is reduced to

$$S_G = \beta_s \sum_s \sum_n \operatorname{ReTr} \left[V(n, s) V^\dagger(n + \mu, s) \right], \tag{7}$$

where the link variable $U_{s,d}(n)$ in the extra direction is regarded as a site variable $V(n, s)(= U_{s,d}(n))$. This action is identical to the one of a $(d - 1)$ -dimensional spin model and s is regarded as an independent flavor. The action eq.(7) is invariant under

$$V(n, s) \longrightarrow g(s)V(n, s)g^\dagger(s+1) \quad , \quad (g(s) \in G), \quad (8)$$

where G is the gauge group of the original model. Therefore the total symmetry of the model is G^{2L_s} , where $2L_s$, the size of the extra dimension, is regarded as the number of independent flavors. We use this (reduced) model for our numerical investigation.

B. Mean field approximation for fermion propagators

When the dynamical gauge fields are added even on the extra dimension only, it is difficult to calculate the fermion propagator analytically. Instead of calculating the fermion propagator *exactly*, we use a mean-field approximation to see an effect of the dynamical gauge field qualitatively. The mean-field approximation we adopt is that the link variables are replaced as

$$V(n, s) \longrightarrow z, \quad (9)$$

where z is a (n, s) -independent constant. From eq.(3) the fermion action in a $(d-1)$ -dimensional momentum space becomes

$$S_F \rightarrow \sum_{s,t,p} \bar{\psi}_s(-p) \left(\sum_{\mu} i\gamma_{\mu} \sin(p_{\mu}) \delta_{s,t} + [M(z)P_R + M^\dagger(z)P_L]_{s,t} \right) \psi_t(p), \quad (10)$$

$$(M(z))_{s,t} = (M_0(z))_{s,t} + \frac{\nabla(p)}{2} \delta_{s,t}, \quad (M^\dagger(z))_{s,t} = (M_0^\dagger(z))_{s,t} + \frac{\nabla(p)}{2} \delta_{s,t}, \quad (11)$$

where $\nabla(p) \equiv \sum_{\mu=1}^{d-1} 2(\cos p_{\mu} - 1)$. Following Ref. [3] it is easy to obtain a mean field fermion propagator on a finite lattice with the periodic boundary condition:

$$\begin{aligned} G(p)_{s,t} &= \left[i \sum_{\mu} \gamma_{\mu} \bar{p}_{\mu} + MP_R + M^\dagger P_L \right]_{s,t}^{-1} \\ &= \left[\left\{ \left(-i \sum_{\mu} \gamma_{\mu} \bar{p}_{\mu} + M \right) G_L(p)_{s,t} \right\} P_L + \left\{ \left(-i \sum_{\mu} \gamma_{\mu} \bar{p}_{\mu} + M^\dagger \right) G_R(p)_{s,t} \right\} P_R \right], \quad (12) \end{aligned}$$

$$G_L(p) = \frac{1}{\bar{p}^2 + M^\dagger M} \quad , \quad G_R(p) = \frac{1}{\bar{p}^2 + MM^\dagger} \quad , \quad (13)$$

with $\bar{p}_\mu = \sin(p_\mu)$. For large L_s where we neglect terms of $O(e^{-cL_s})$ with $c > 0$, G_L and G_R are given by

$$[G_L(p)]_{s,t} = \begin{cases} Be^{-\alpha_+|s-t|} + (A_L - B)e^{-\alpha_+(s+t)} + (A_R - B)e^{-\alpha_+(2L_s-s-t)}, & (s, t \geq 0) \\ A_L e^{-\alpha_+s+\alpha_-t} + A_R e^{-\alpha_+(L_s-s)-\alpha_-(L_s+t)}, & (s \geq 0, t \leq 0) \\ A_L e^{\alpha_-s-\alpha_+t} + A_R e^{-\alpha_-(L_s+s)-\alpha_+(L_s-t)}, & (s \leq 0, t \geq 0) \\ Ce^{-\alpha_-|s-t|} + (A_L - C)e^{\alpha_-(s+t)} + (A_R - C)e^{-\alpha_-(2L_s+s+t)}, & (s, t \leq 0) \end{cases} \quad (14)$$

$$[G_R(p)]_{s,t} = \begin{cases} Be^{-\alpha_+|s-t|} + (A_R - B)e^{-\alpha_+(s+t+2)} + (A_L - B)e^{-\alpha_+(2L_s-s-t-2)}, & (s, t \geq -1) \\ A_R e^{-\alpha_+(s+1)+\alpha_-(t+1)} + A_L e^{-\alpha_+(L_s-s-1)-\alpha_-(L_s+t+1)}, & (s \geq -1, t \leq -1) \\ A_R e^{\alpha_-(s+1)-\alpha_+(t+1)} + A_L e^{-\alpha_-(L_s+s+1)-\alpha_+(L_s-t-1)}, & (s \leq -1, t \geq -1) \\ Ce^{-\alpha_-|s-t|} + (A_R - C)e^{\alpha_-(s+t+2)} + (A_L - C)e^{-\alpha_-(2L_s+s+t+2)}, & (s, t \leq -1) \end{cases} \quad (15)$$

where

$$a_\pm = z\left(1 - \frac{\nabla(p)}{2} \mp m_0\right) = zb_\pm, \quad (16)$$

$$\alpha_\pm = \operatorname{arccosh} \left[\frac{\bar{p}^2 + z^2 + b_\pm^2}{2zb_\pm} \right], \quad (17)$$

$$A_L = \frac{1}{a_+e^{\alpha_+} - a_-e^{-\alpha_-}}, \quad A_R = \frac{1}{a_-e^{\alpha_-} - a_+e^{-\alpha_+}}, \quad (18)$$

$$B = \frac{1}{2a_+ \sinh \alpha_+}, \quad C = \frac{1}{2a_- \sinh \alpha_-}. \quad (19)$$

Behaviors of A_R , B and C as $p \rightarrow 0$ are similar to the ones in free theory: They have no singularity for all z . A behavior of A_L is, however, different: As $p \rightarrow 0$ A_L behaves as

$$A_L \rightarrow \frac{1}{[(1-m_0)^2] + O(p^2)}, \quad (0 < m_0 < 1-z), \quad (20)$$

$$\rightarrow \frac{4m_0^2 - [(z^2-1) - m_0^2]^2}{4m_0z^2p^2}, \quad (1-z < m_0 < 1). \quad (21)$$

A critical value of the domain-wall mass that separates a region with a zero mode and a region without zero modes is $m_0^c = 1 - z$. Since A_L term dominates for $1 - z < m_0 < 1$ in

the G_L (eq.(14)) and G_R (eq.(15)), a right-handed zero mode appears in the $s = 0$ plane , and a left-handed zero mode in the $s = L_s - 1$ plane. For $0 < m_0 < 1 - z$ the right- and left-handed fermions are massive in all s planes. Since the terms of A_L, A_R, B and C are almost same value in this region of m_0 , a translational invariant term dominates in G_L and G_R , so that the spectrum becomes vector-like.

If $z \rightarrow 1$, the model becomes free theory. The propagator obtained in this section agrees with the one obtained in Ref. [3]. In the opposite limit that $z \rightarrow 0$, since there is no hopping term to the neighboring layers, this model becomes the one analyzed in Ref. [13] in the case of the strong coupling limit $\beta_s = 0$, and in Ref. [14] , in the case that z is identified to the vacuum expectation value of the link variables. This consideration suggests that the region where the zero modes exist become smaller and smaller as z ($1 - z < m_0 < 1$) approaches zero. What corresponds to z ? Boundary conditions z satisfies are $z = 1$ at $\beta_s = \infty$ and $z = 0$ at $\beta_s = 0$. The most naive candidate [14] is

$$z = \langle V(n, s) \rangle. \quad (22)$$

But this is not invariant under the symmetry (8). The other choice invariant under (8) is

$$z^2 = \langle \text{TrRe}\{V(n, s)V^\dagger(n + \mu, s)\} \rangle. \quad (23)$$

If eq. (22) is true, zero modes disappears in the symmetric phase, where $\langle V(n, s) \rangle = 0$, while, for the case of eq. (23), the zero modes always exist in both phases, since $\langle \text{TrRe}\{V(n, s)V^\dagger(n + \mu, s)\} \rangle$ is insensitive to which phase we are in.

III. NUMERICAL STUDY OF (2+1)-DIMENSIONAL U(1) MODEL

A. Method of numerical calculations

In this section we numerically study the domain-wall model in $(2 + 1)$ -dimension with a $U(1)$ dynamical gauge field in the extra dimension. As seen from eq.(7) , the gauge

field action can be identified with a 2-dimensional $U(1)$ spin model (with $2L_s$ copies). In $(2 + 1)$ -dimension, γ -matrices are Pauli-matrices , σ_1 , σ_2 , σ_3 .

Our numerical simulation has been carried out by the quenched approximation. Configurations of $U(1)$ dynamical gauge field are generated and fermion propagators are calculated on the configurations. The obtained fermion propagators are gauge non-invariant in general under the symmetry (8). The fermion propagator $G(p)_{s,t}$ becomes “invariant” if and only if $s = t$. Thus, we take the $s - s$ layer as propagating plane(\approx “physical space”), and investigate the behavior of the fermion propagator in this layer.

To study the fermion spectrum, we assume a form of eq.(12) for the fermion propagator, from which we extract G_L and G_R . We then obtain corresponding fermion masses from $G_L^{-1}(p)$ and $G_R^{-1}(p)$ by fitting them linearly in \bar{p}^2 , since, from eq.(13) :

$$G_L^{-1} = \bar{p}^2 + M^\dagger M \rightarrow m_f^2 \quad , \quad (p \rightarrow 0), \quad (24)$$

$$G_R^{-1} = \bar{p}^2 + M M^\dagger \rightarrow m_f^2 \quad , \quad (p \rightarrow 0). \quad (25)$$

We take the following setup for 2-dimensional momenta. A periodic boundary condition is taken for the 1st direction and the momentum in this direction is fixed on $p_1 = 0$. An anti-periodic boundary condition is taken for the 2nd-direction and the momentum in this direction is variable such as $p_2 = (2n + 1)\pi/L$, $n = -L/2, \dots, L/2 - 1$.)

If $m_f^2 = 0$, we conclude that there is a zero mode, and if $m_f^2 \neq 0$, there is not.

B. Simulation parameters

Our simulation is performed in the quenched approximation on $L^2 \times 2L_s$ lattices with $L = 16, 24, 32$ and $L_s = 16$. The coordinate s in the extra dimension runs $-16 < s < 15$. Gauge configurations are generated by the 5-hit Metropolis algorithm at $\beta_s = 0.5, 1.0, 5.0$. For the thermalization first 1000 sweeps are discarded.

The fermion propagators are calculated by the conjugate gradient method on 50 configurations separated by at least 20 sweeps, except at $\beta_s = 5.0$ on a $32^2 \times 32$ lattice where

the number of configurations are 11. We take the domain-wall mass $m_0 = 0.7, 0.8, 0.9, 0.99$ at $\beta_s = 0.5$, $m_0 = 0.3, 0.4, 0.5, 0.6, 0.9$ at $\beta_s = 1.0$, and $m_0 = 0.1, 0.2, 0.3$ at $\beta_s = 5.0$. The boundary conditions in 1st- and 3rd(extra)-directions are periodic and the one in 2nd-direction is anti-periodic. Wilson parameter r has been set to $r = 1$. The fermion propagators have been investigated at $s = 0, 8, 15$. These s are the layers where we put sources. The layer at $s = 0$ is the domain-wall, at $s = 15$, the anti-domain-wall, and at $s = 8$, neither. Errors are all estimated with the jack-knife method.

C. Quenched phase structure

As explained before the gauge field action of our model is identical to that of the $U(1)$ spin system in 2-dimensions. Therefore, there is a Kosterlitz-Thouless phase transition and this system does not have an order parameter on the infinite lattice. On the finite volume, however, we take a vacuum expectation value of link variables as an order parameter using rotation technique:

$$v = \langle \left| \frac{1}{L^2} \sum_n V(n, s) \right| \rangle_s, \quad (26)$$

where L is the lattice size of the 1, 2-dimension.

The defined vacuum expectation value v above is zero in the Kosterlitz-Thouless phase but $v > 0$ in the spin-wave phase on the finite lattice. (Increasing the lattice size, however, decreasing the value of v . In the infinite lattice size, the value of v is zero for all gauge coupling.) Since we are interested in the dynamics of 4-dimensional theories, where the phase transition separates a symmetric phase from a broken phase, we have used this 2-dimensional system on large but finite volume as a toy model of 4-dimensional real world. Therefore, in this letter, we refer to the Kosterlitz-Thouless phase as the symmetric phase, and to the spin-wave phase as the broken phase. Fig. 1(a) shows that, on a $16^2 \times 32$ lattice, v behaves as if it was an order parameter. From Fig. 1(b) we consider that the system is in the symmetric phase at $\beta_s = 0.5$, while in the broken phase at $\beta_s = 1.0, 5.0$.

D. Fermion spectrum in the broken phase

At $\beta_s = 1.0$ and 5.0 , the system is in broken phase. Here we mainly discuss the result at $\beta_s = 1.0$ in detail.

We first consider the fermion spectrum on the layer at $s = 0$. Fig. 2 is a plot of the term corresponding to $-\sin(p_2) \cdot G_L$ and $-\sin(p_2) \cdot G_R$ as a function of p_2 at $m_0 = 0.3$ and 0.5 . (Note we always set $p_1 = 0$.) This figure shows that, as p_2 goes to zero, G_L seems to diverge at $m_0 = 0.5$ but stay finite at $m_0 = 0.3$, while G_R stays finite at both m_0 . Next let us show Fig. 3, which is a plot of the G_L^{-1} and G_R^{-1} as a function of $\bar{p}_2^2 \equiv \sin^2(p_2)$ at $m_0 = 0.3$ and 0.5 . In the limit $p_2 \rightarrow 0$, G_R^{-1} remains non-zero at both m_0 , while G_L^{-1} vanishes at $m_0 = 0.5$. We obtain the value of m_f^2 , which can be regarded as the mass square in 2-dimensional world, by the linear fit in \bar{p}_2^2 , and plot m_f as a function of m_0 in Fig. 4. The mass of right-handed fermion, obtained from G_L^{-1} , becomes very small (less than 0.1) at m_0 larger than 0.5, so we conclude that this critical value is $m_0^c \sim 0.5$. Whenever the domain-wall mass is larger than this value, this model produces the right-handed chiral zero mode on the domain-wall at $s = 0$.

On the anti-domain-wall ($s = 15$), on the other hand, the mass of left-handed fermion becomes less than 0.1 at m_0 larger than the critical mass $m_0^c \sim 0.5$, as seen in Fig. 5. It is noted that chiralities between the zero modes on the domain-wall and the anti-domain-wall are opposite each other.

Finally Fig. 6 shows that, on $s = 8$, the layer in the middle between the domain-wall and the anti-domain-wall, both right-handed and left-handed fermions stay heavy.

A similar result at $\beta_s = 5.0$ on $s = 0$ is given Fig. 7.

From these results above, we conclude that the domain-wall model with the dynamical gauge field on the extra dimension (*i.e.* the weak coupling limit of the original Kaplan's model) can create the chiral zero mode on the domain-wall, at least in the broken phase. This suggests that the original Kaplan's model has a great chance to work for the construction of lattice chiral gauge theories in the broken phase.

E. Fermion spectrum in symmetric phase

The system is in the symmetric phase at $\beta_s = 0.5$. The fermion propagator is analyzed in the same way as in the broken phase. However, for example on the $s = 0$ layer, $-\sin(p_2) \cdot G_L$ and $-\sin(p_2) \cdot G_R$ show similar behaviors on a $16^2 \times 32$ lattice, as seen in Fig. 8. Smaller lattice sizes, stronger the similarity, which makes analysis more difficult in the symmetric phase. To see a difference between the right-handed and left-handed fermions, we have to take larger lattice size such as $L = 24, 32$.

In Fig. 9, we have plotted mass m_f of both modes at $s = 0$ as a function of m_0 . Although a difference of masses between the right-handed and the left-handed fermions is very small, about 0.1 or less at $m_0 = 0.99$, this difference stays finite as we increase the spatial lattice size L from 24 to 32. Therefore we conclude that the right-handed fermion becomes massless at m_0 larger than 0.9, while the left-handed fermion stays massive at all m_0 , so that the fermion spectrum on the domain-wall is *chiral*.

In order to see that the difference of mass between the right and the left is really a signal, not a statistical fluctuation, we have plotted m_f vs. m_0 in the case of putting a source at the anti-domain-wall $s = 15$ in Fig. 10. We observe, at $m_0 = 0.99$, a massless fermion of the opposite chirality to the $s = 0$ zero mode and a finite difference of masses between the right and the left, which stays finite as we increase the spatial lattice size.

Furthermore, in the case of $s = 8$, the right-handed fermion and the left-handed fermion stay massive at all m_0 , as seen in Fig. 11

From these results above, as the same case in the broken phase, we conclude that the original Kaplan's model can create the chiral zero mode on the domain-wall even in the symmetric phase.

IV. CONCLUSIONS AND DISCUSSIONS

Using the quenched approximation, we have performed the numerical study of the domain-wall model in (2+1)-dimensions with the $U(1)$ dynamical gauge field on the extra dimension. From this study we obtain the following results. There exists the critical value of the domain-wall mass separating the region with a chiral zero mode and the region without it, both in the broken and the symmetric phases of the gauge field. At the domain-wall mass larger than its critical value a zero mode with one chirality exists on the domain-wall and a zero modes with opposite chirality on the anti-domain-wall, and none in the middle between the domain-wall and the anti-domain-wall.

These results strongly suggest that it is possible to construct lattice chiral gauge theories at all β_s except for $\beta_s = 0$ via the domain-wall method, and continuum limits may possibly be taken at the critical value of β_s where the phase transition takes place. In (2+1)-dimensions, however, the gauge field in $\beta = \infty$ limit is special since there is no order parameter and the phase transition is topological. Thus, to make a definite conclusion on the construction of lattice chiral gauge theories via the domain-wall method, we must study realistic (4 + 1)-dimensional model with $U(1)$ or $SU(N)$ gauge field in $\beta = \infty$ limit. Such models in $\beta = \infty$ limit have a phase transition characterized by an order parameter, a vacuum expectation value of the link variables in the extra dimension.

Moreover, it is interesting and important to find an appropriate correspondence between the propagator obtained in the numerical simulation and the mean field propagator with tuned parameter z . So far it is not clear what physical quantity is corresponding to z . Since zero mode seems to exist even in the symmetric phase, the correspondence (22) is qualitatively incorrect. On the other hand, we have found that the correspondence (23) fails to reproduce m_0^c quantitatively. Since mean-field approximations can not work well in the lower-dimensions in general, we must try to answer these questions studying (4 + 1)-dimensional $U(1)$ or $SU(N)$ models.

ACKNOWLEDGEMENTS

Numerical calculations for the present work have been carried out at Center for Computational Physics, University of Tsukuba. This work is supported in part by the Grants-in-Aid of the Ministry of Education(Nos. 04NP0701, 06740199).

REFERENCES

- [1] H. B. Nielsen and M. Ninomiya, Nucl. Phys. **B185**, 20 (1981) ; Nucl. Phys. **B193**, 173 (1981); Phys. Lett. **B105**, 219 (1981);
L. H. Karsten, Phys. Lett. **B104**, 315 (1981).
- [2] D. B. Kaplan, Phys. Lett. **B288**, 342 (1992).
- [3] S. Aoki and H. Hirose, Phys. Rev. **D49**, 2604 (1994).
- [4] K. Jansen, Phys. Lett. **B301**, 219 (1992).
- [5] R. Narayanan and H. Neuberger, Phys. Lett. **B302**, 62 (1993).
- [6] R. Narayanan and H. Neuberger, Nucl. Phys. **B412**, 574 (1994).
- [7] M. F. L. Golterman, K. Jansen, D. N. Petcher, and J. C. Vink, Phys. Rev. **D49**, 1606 (1994);
M. F. L. Golterman and Y. Shamir, Phys. Rev. **D51**, 3026 (1995).
- [8] R. Narayanan and H. Neuberger, Nucl. Phys. **B443**, 305 (1995);
R. Narayanan , H. Neuberger and P. Vranas, Phys. Lett. **353B**, 507 (1995) ;
T. Kawano and Y. Kikukawa, preprint KUNS-1317 Jan 1995.
- [9] S. Aoki and R. B. Levien, Phys. Rev. **D51**, 3790 (1995).
- [10] Y. Shamir, Nucl. Phys. **B417** 167 (1994).
- [11] M. F. L. Golterman and Y. Shamir, Phys. Lett. **B353**, 84 (1995).
- [12] R. Narayanan and H. Neuberger, preprint RU-95-49 Jul 1995.
- [13] H. Aoki, S. Iso, J. Nishimura, and M. Oshikawa, Mod. Phys. Lett. **A9**, 1755 (1994).
- [14] C. P. Korthals-Altes, S. Nicolis, and J. Prades, Phys. Lett. **B316**, 339 (1993).

FIGURES

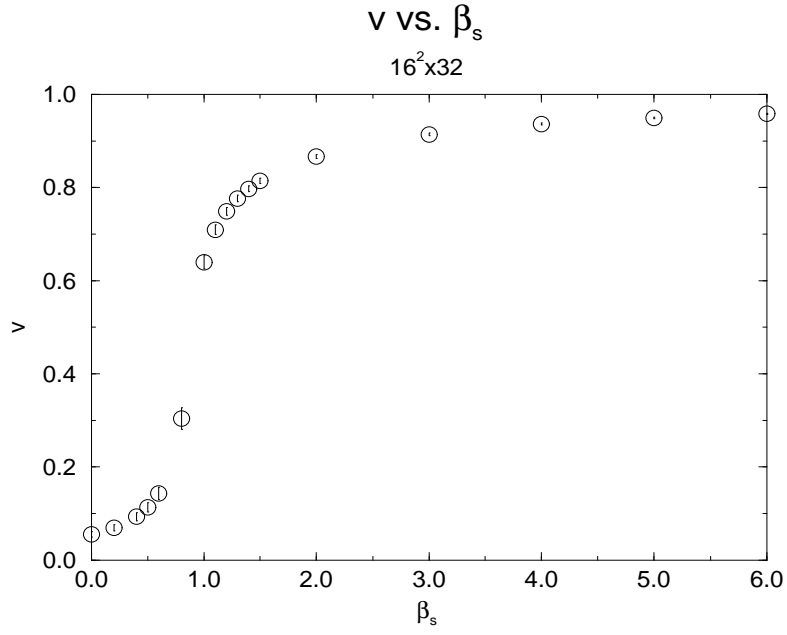


Fig. 1(a)

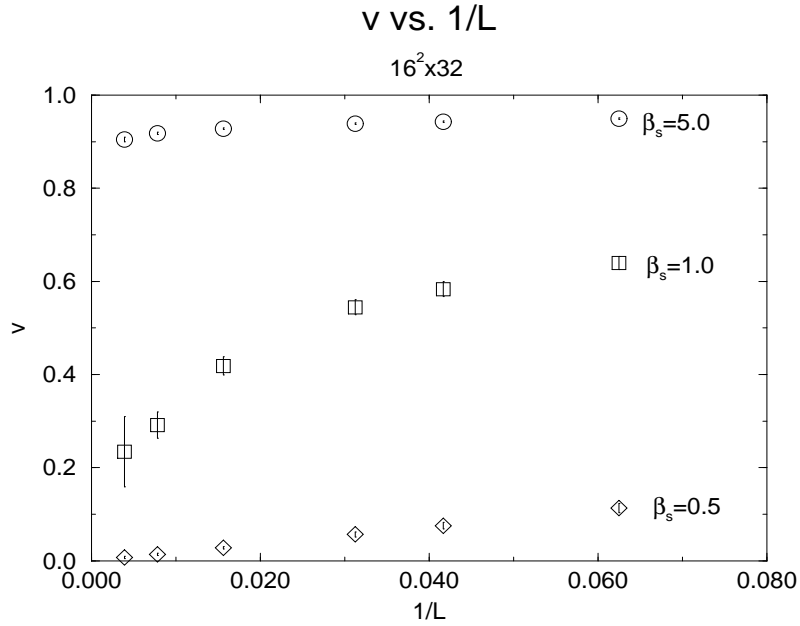


Fig. 1(b)

FIG. 1. (a) Vacuum expectation value of link variables v on a $16^2 \times 32$ lattice as a function of β_s . (b) A volume dependence of the vacuum expectation values of link variables v as a function of $1/L$.

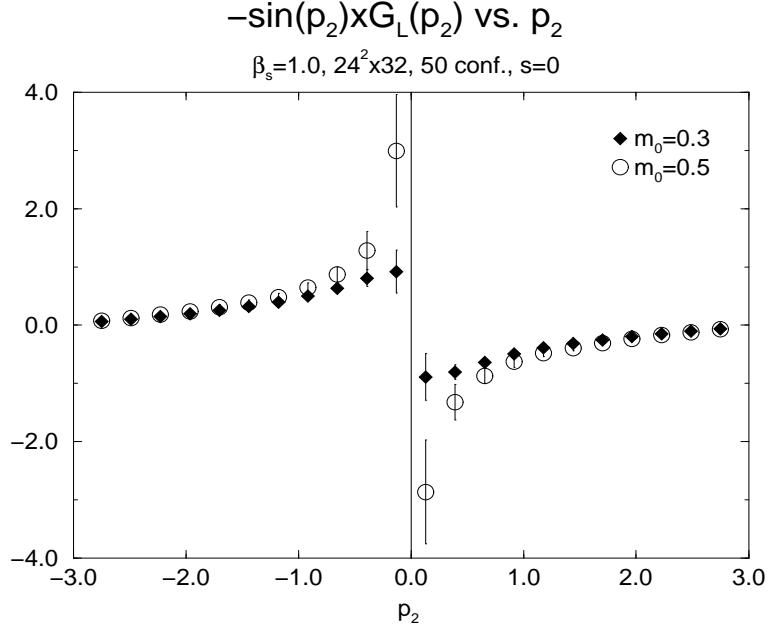


Fig. 2(a)

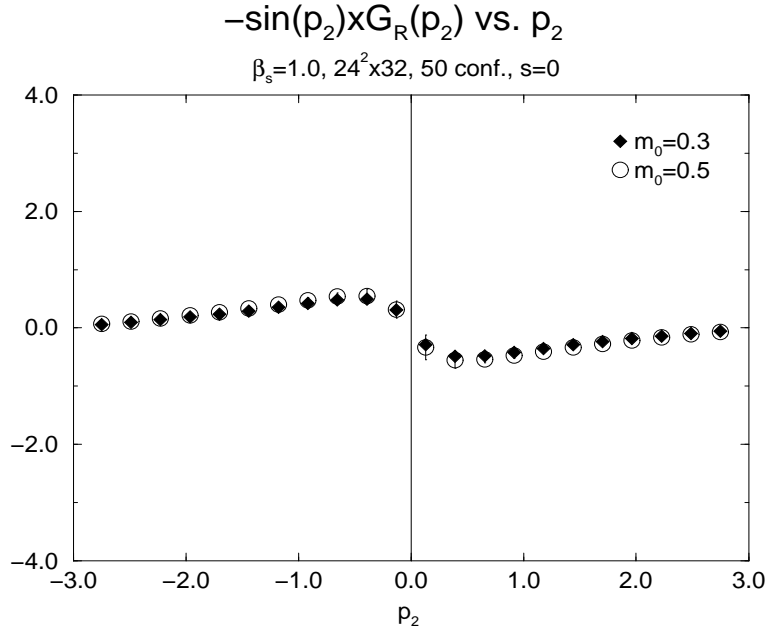


Fig. 2(b)

FIG. 2. $-\sin(p_2) \cdot [G_L]_{0,0}$ and $-\sin(p_2) \cdot [G_R]_{0,0}$ in the fermion propagator as a function of p_2 with $p_1 = 0$ at $\beta_s = 1.0$ on a $24^2 \times 32$ lattice, for $m_0=0.5$ (open circles) and 0.3 (solid diamonds).

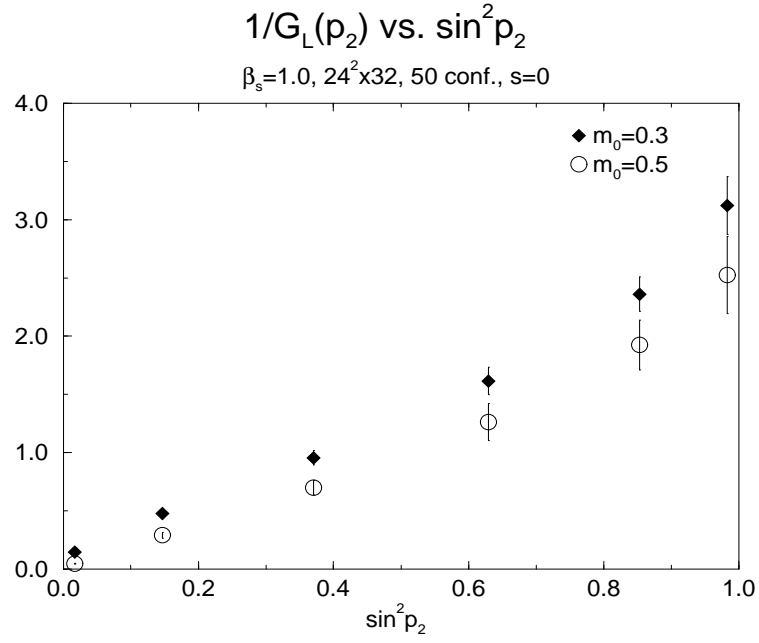


Fig. 3(a)

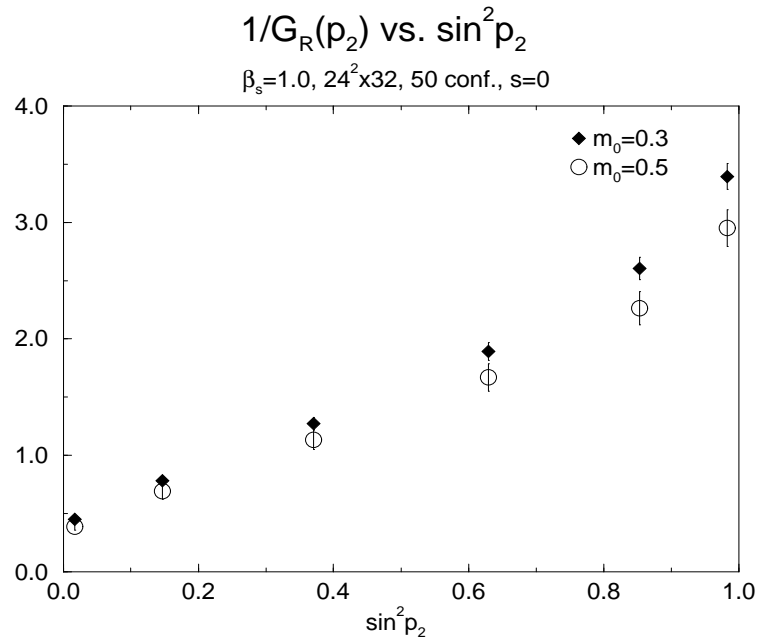


Fig. 3(b)

FIG. 3. $[G_L]_{0,0}^{-1}$ and $[G_R]_{0,0}^{-1}$ as a function of $\sin^2(p_2)$ with $p_1 = 0$ at $\beta_s = 1.0$ on a $24^2 \times 32$ lattice, for $m_0=0.5$ (open circles) and 0.3 (solid diamonds).

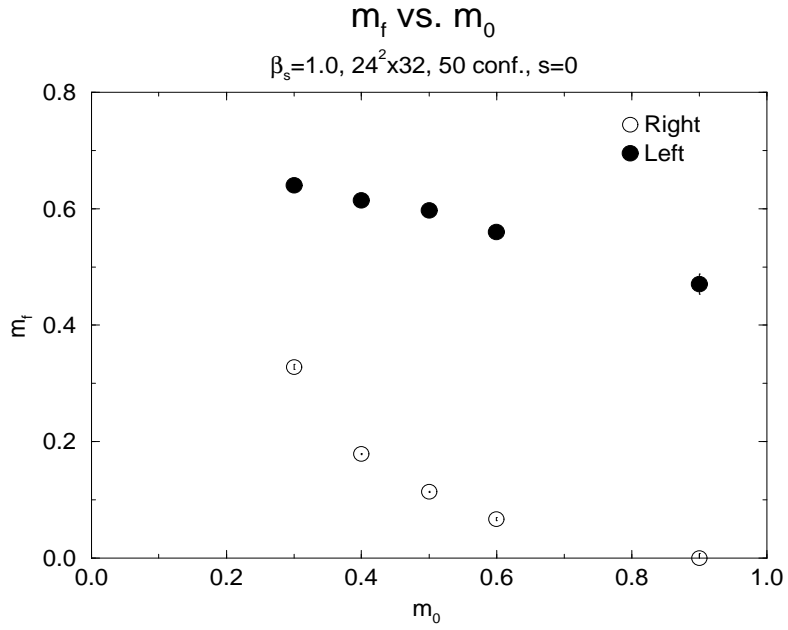


Fig. 4

FIG. 4. m_f vs. m_0 at $\beta_s = 1.0$ on a $24^2 \times 32$ lattice, in the case of putting a source on the domain-wall $s = 0$, for the right-handed fermion (open circles) and the left-handed fermion (solid circles).

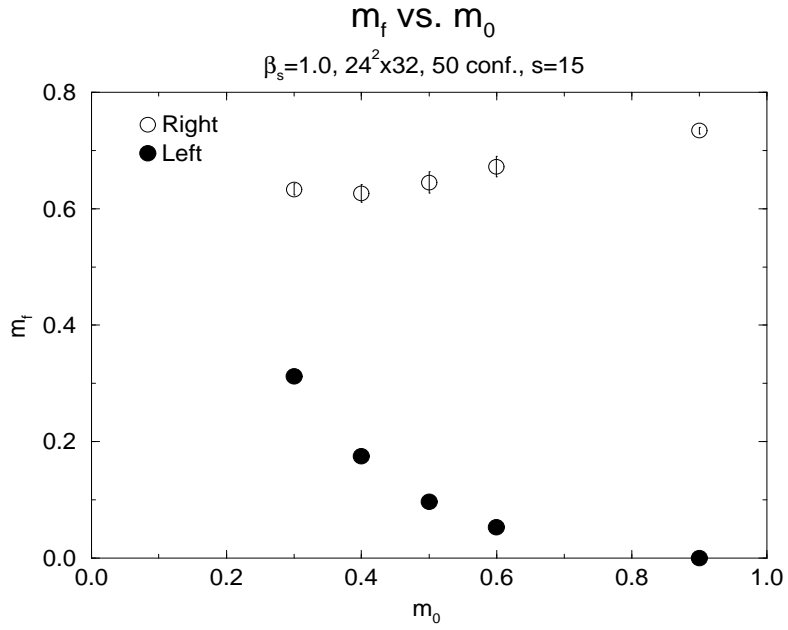


Fig. 5

FIG. 5. m_f vs. m_0 at $\beta_s = 1.0$ on a $24^2 \times 32$ lattice, in the case of putting a source on the anti-domain-wall $s = 15$, for the right-handed fermion (open circles) and the left-handed fermion (solid circles).

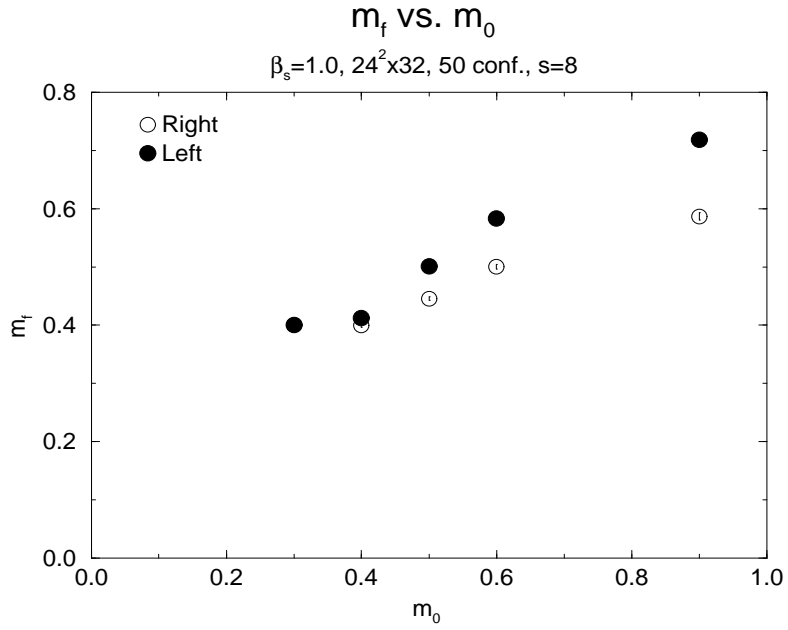


Fig. 6

FIG. 6. m_f vs. m_0 at $\beta_s = 1.0$ on a $24^2 \times 32$ lattice, in the case of putting a source on $s = 8$, for the right-handed fermion (open circles) and the left-handed fermion (solid circles).

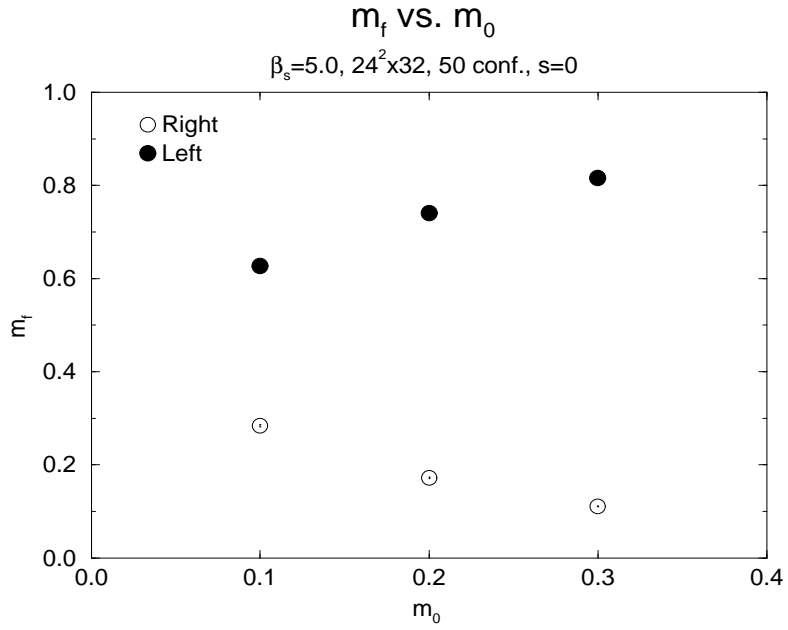


Fig. 7

FIG. 7. m_f vs. m_0 at $\beta_s = 5.0$ on a $24^2 \times 32$ lattice, in the case of putting a source on the domain-wall $s = 0$, for the right-handed fermion (open circles) and the left-handed fermion (solid circles).

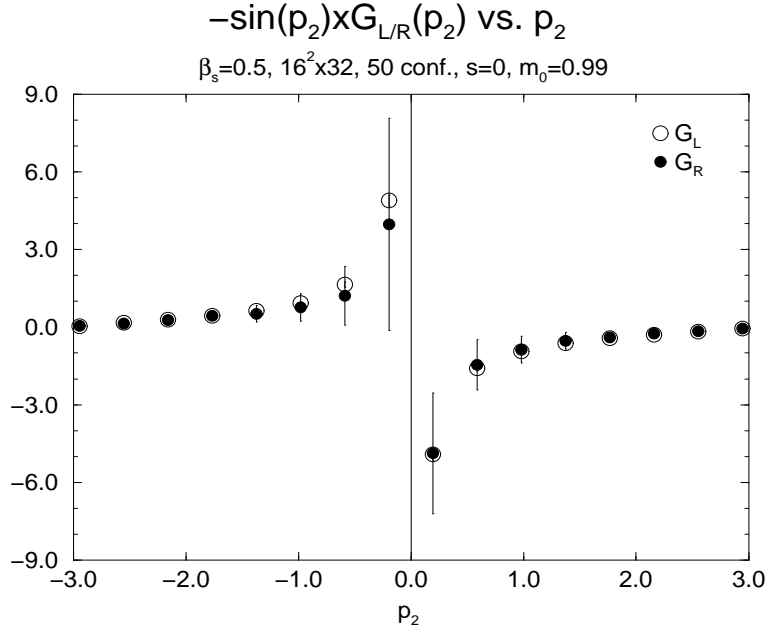


Fig. 8

FIG. 8. $-\sin(p_2) \cdot [G_L]_{0,0}$ (open circles) and $-\sin(p_2) \cdot [G_R]_{0,0}$ (solid circles) as a function of p_2 with $p_1 = 0$ at $\beta_s = 0.5$ on a $16^2 \times 32$ lattice.

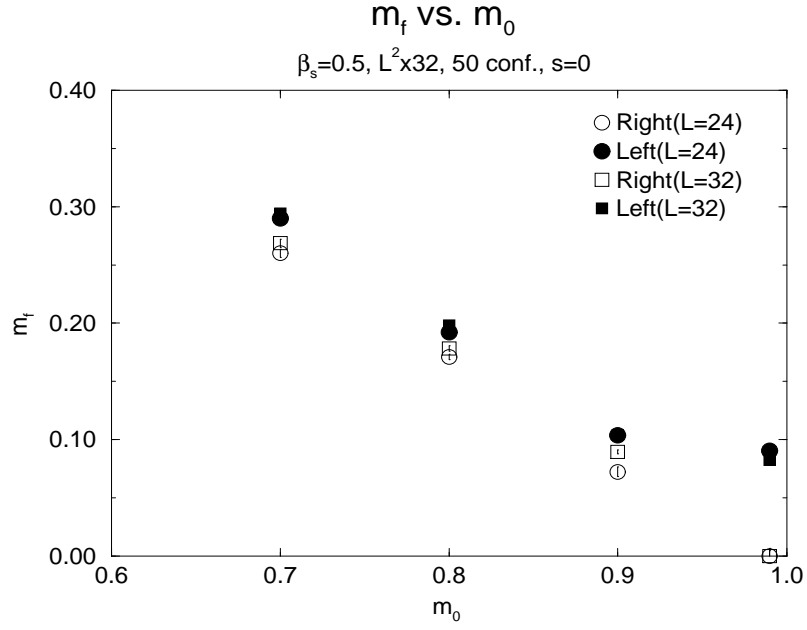


Fig. 9

FIG. 9. m_f vs. m_0 at $\beta_s = 0.5$ on $L^2 \times 32$ lattices with $L = 24$ (circles) and 32 (squares) in the case of putting a source on the domain-wall $s = 0$. Open symbol stands for the right-handed fermion and Solid symbol for the left-handed fermion.

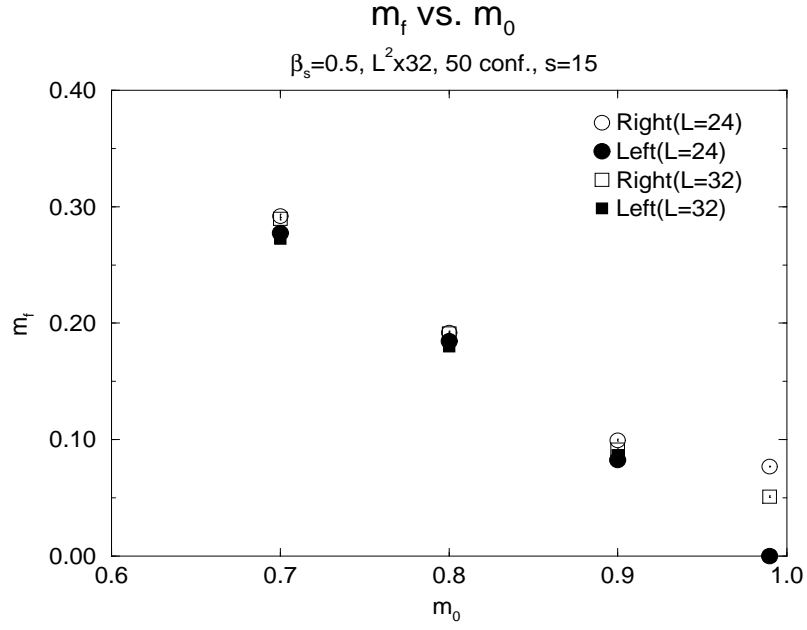


Fig. 10

FIG. 10. m_f vs. m_0 at $\beta_s = 0.5$ on $L^2 \times 32$ lattices with $L = 24$ (circles) and 32 (squares) in the case of putting a source on the anti-domain-wall $s = 15$. Open symbol stands for the right-handed fermion and Solid symbol for the left-handed fermion.

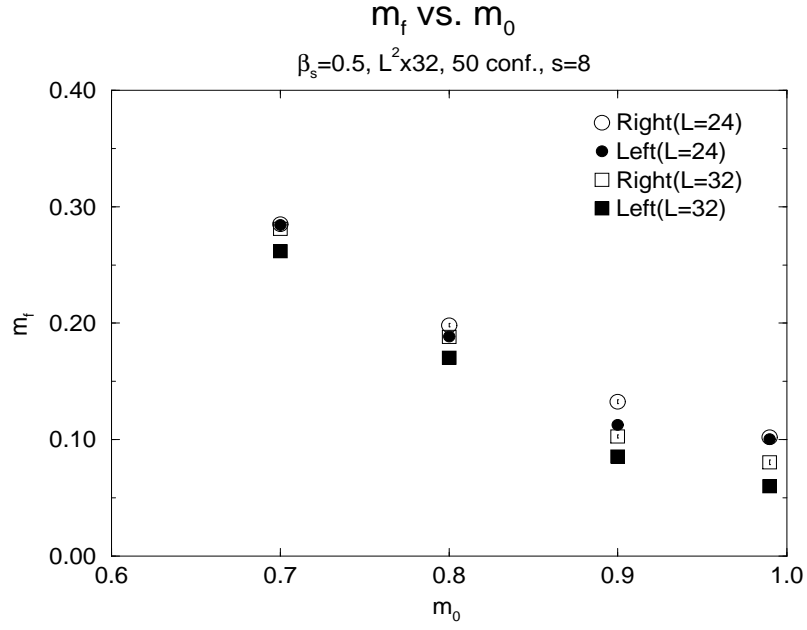


Fig. 11

FIG. 11. m_f vs. m_0 at $\beta_s = 0.5$ on $L^2 \times 32$ lattices with $L = 24$ (circles) and 32 (squares) in the case of putting a source on $s = 8$. Open symbol stands for the right-handed fermion and Solid symbol for the left-handed fermion.